Unified Theory of Oscillator Phase Noise I: White Noise

William Loh, *Student Member, IEEE*, Siva Yegnanarayanan, *Member, IEEE*, Rajeev J. Ram, *Senior Member, IEEE*, and Paul W. Juodawlkis, *Senior Member, IEEE*

***Abstract*—The spectral purity of every oscillator system is limited by phase noise. In this work, we extend the techniques previously used to analyze phase noise in lasers to develop an intuitive, yet powerful description of phase noise in an electromagnetic oscillator for the case when the oscillating field is sinusoidal and perturbed by white noise. The developed theory is general and unifies the understanding of phase noise in both electrical and optical oscillators. Our approach is based on partitioning the noise among the modes of the oscillator, which is analogous to the approach used to analyze phase noise in laser cavities, but has not been previously considered for electrical oscillators. We show that oscillator phase noise depends only on the oscillating power, injected noise, and round-trip delay. This result provides a theoretical foundation to and expands upon the predictions provided by Leeson's well-known empirical oscillator phase-noise model. To validate the developed theory, we compare the predicted phase noise to the experimentally measured phase noise of both a simple electrical oscillator and a hybrid opto-electronic oscillator and show excellent agreement across a wide range of operation.**

***Index Terms*—Microwave photonics (MWPs), oscillators, phase noise, RF, white noise.**

I. Introduction

OSCILLATORS are essential components enabling operation for a wide variety of systems. Their applications span multiple disciplines of science, and their use is ubiquitous at frequencies ranging from optical to microwave and below. A solid understanding of oscillator operation is critical for the modeling and design of future oscillator-based systems.

The most important property that characterizes oscillator performance is phase noise. Due to an oscillator's intrinsic negative feedback (maintaining gain = loss) and to various amplitude-limiting components in the system (e.g., the saturated amplifier), the low-frequency amplitude noise is typically greatly suppressed relative to phase noise. As the primary function of many oscillators is to generate a pure sinusoid, the phase noise acts to degrade operation by spreading the oscillator power across a range of frequencies.

Over the last several decades, significant research has been devoted toward understanding the problem of oscillator phase noise. The simplest theories represent the oscillator as a linear time-invariant (LTI) system and consider the oscillator's output as a resonant response to input noise [1], [2]. Although intuitive, these theories do not account for the randomness in the phase of noise upon each addition of noise to the oscillator field. The relative phase between the signal field and the added noise results in separation of the noise perturbation into quadratures of amplitude and phase, forming the basis for linear time-variant (LTV) analysis as applied in [3] and [4]. The linearization of the oscillator phase in [3] and [4], however, introduces nonphysical artifacts of infinite spectral power at frequencies approaching the carrier. In an alternative description of an oscillator using a rigorous stochastic differential equation, [5] and [6] apply Floquet theory to show the oscillator spectrum to be a Lorentzian for white-noise perturbation. The Lorentzian distribution [5]–[10] establishes the power at the oscillation frequency to be finite, relieving predictions of infinite power [1], [3]. Although the approach of [5] and [6] is rigorous, its resulting solution is nonintuitive and difficult to apply, as it requires detailed analysis of the oscillator dynamics, e.g., the determination of the Floquet eigenvectors. Ideally, one desires a simple and intuitive functional description of oscillator phase noise, similar to the empirical model proposed by Leeson [1], but based on physics fundamental to the behavior of an oscillator [5], [6]. Due to the many parallels that exist between electrical and optical oscillators, one would desire this description to be general so as to encompass the operation of oscillators across both disciplines.

In this work, we present a novel and general approach to the description of phase noise when the oscillator field is sinusoidal and perturbed by additive white noise. Our theory is intuitive and expands upon the method of vector addition used by Henry [9] to describe the linewidth of semiconductor lasers. This approach is consistent with the use of LTV analysis, but does not impose linearization of the oscillator's phase in the steady state. To improve upon existing theories, we also introduce a concept of noise partitioning to treat the interaction of noise with the oscillating field. Our formulation is based on the observation that the continuum representation of noise outside the oscillator becomes an inappropriate description of noise within the confines of the oscillator boundaries. The noise generated must instead be coupled into the modes of the resonant system, which together form the basis of the oscillator. The amount of noise

Manuscript received November 02, 2012; revised March 29, 2013; accepted April 02, 2013. Date of publication May 06, 2013; date of current version May 31, 2013. This work was supported in part by the Assistant Secretary of Defense for Research and Engineering under Air Force Contract FA8721-05-C-0002.

W. Loh is with the Electrical Engineering Department, Massachusetts Institute of Technology (MIT), Cambridge, MA 02139 USA, and also with the MIT Lincoln Laboratory, Lexington, MA 02420 USA (e-mail: william.loh@ll.mit.edu).

S. Yegnanarayanan and P. W. Juodawlkis are with the MIT Lincoln Laboratory, Lexington, MA 02420 USA (e-mail: siva.yegnanarayanan@ll.mit.edu; juodawlkis@ll.mit.edu).

R. J. Ram is with the Electrical Engineering Department, Massachusetts Institute of Technology, Cambridge, MA 02139 USA (e-mail: rajeev@mit.edu).

Color versions of one or more of the figures in this paper are available online at http://ieeexplore.ieee.org.

Digital Object Identifier 10.1109/TMTT.2013.2260170

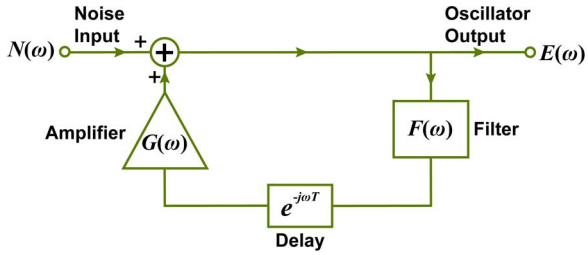

Fig. 1. Block diagram illustration of phase noise in an oscillator consisting of an amplifier, delay line, and filter wrapped in a positive feedback circuit.

coupling into each mode is modified by the density of modes, as has been well established in laser physics [10]–[20]. We note that the restriction of our present analysis to white-noise perturbation prevents full application of the theory to oscillators that exhibit noise of $1/f^{\alpha}$ characteristics. However, the foundations provided here should prove helpful for understanding oscillator behavior under noise perturbation of arbitrary form. We are currently working toward the generalization of this analysis to $1/f^{\alpha}$ noise [21]. A central underlying theme for the work presented here is the unification in the understanding of phase noise for both electrical and optical oscillators. Toward that end, we show that our general theory of phase noise is consistent with well-established models of laser linewidth [7], [9], [10]. We also support our theory by measuring the phase noise of electrical oscillators and show excellent agreement over a wide range of operation. We conclude by comparing the theory to the measured phase noise of a hybrid opto-electronic oscillator (OEO) [2], [22]–[24] to further demonstrate the generality of the theory.

II. Review of LTI Phase-Noise Theory

Before presenting our developed theory, we wish to briefly review existing LTI models of phase noise. This section will also serve to highlight the broad range of oscillators our theory is applicable to.

Fig. 1 shows a block diagram of a generic oscillator operating by means of positive feedback. The amplifier noise $(N(\omega))$ is taken to be the system input that is delayed $(e^{-j\omega T})$, amplified (net gain $G(\omega)$), and filtered (transfer function $F(\omega)$) on each round-trip of the oscillator. Note that the delay does not have to be purely a physical delay, and in this case, includes the group delay accumulated from signal propagation through the filter resonance. Despite its inherent simplicity, the system of Fig. 1 represents the general equivalent circuit for many types of oscillators. One example is a *LC* oscillator where the amplifier and system delay retain their usual definitions, and the *LC* resonator forms the equivalent filter.

We are interested in applying LTI analysis to the oscillator of Fig. 1. In addition to noise amplification, there is also reinjection of noise on every round-trip with round-trip time T. The system output can then be formulated as

$$\begin{aligned} E(\omega) &= N(\omega) + N(\omega)G'(\omega)e^{-j\omega T} + N(\omega)G'(\omega)^2e^{-j2\omega T} \\ &\quad + \cdots \\ &= \frac{N(\omega)}{1 - G'(\omega)e^{-j\omega T}} \end{aligned} \tag{1}$$

where $G'(\omega) = G(\omega)F(\omega)$ represents the cascaded amplitude response of the amplifier and filter. Equation (1) is the classic result derived from feedback analysis with the contributions of noise reinjection explicitly highlighted. To calculate the normalized spectrum, we multiply (1) by $E(\tilde{\omega})^*$, take the ensemble average, integrate over $\tilde{\omega}$ [10], and divide the result by the signal power (P_{sig}) yielding

$$\frac{S_E(\omega)}{P_{\text{sig}}} = \frac{S_N(\omega)}{P_{\text{sig}}} \frac{1}{1 + G'(\omega)^2 - 2G'(\omega)\cos(\omega T)}. \tag{2}$$

In (2), $S_E(\omega)$ represents the spectral density of the output field, while $S_N(\omega)$ denotes the spectral density of the noise process itself. Under steady-state conditions, $G'(\omega)$ approaches the value of unity at the oscillation frequency. Equation (2) thus shows that modes are formed at the oscillator resonance frequencies $(\omega T = 2m\pi)$ where m is a non-negative integer. Expanding (2) around a single resonance results in

$$\frac{S_E(\omega)}{P_{\text{sig}}} = \frac{S_N(\omega)}{P_{\text{sig}}} \frac{1}{\Delta\omega^2 T^2} \tag{3}$$

where we have taken $G'(\omega) = 1$ for small $\Delta\omega$. Here, $\Delta\omega$ is the offset angular frequency around the carrier. Equation (3) is analogous to standard results from LTI models of phase noise [1]–[4]. Note that the divergence of the spectrum at $\Delta\omega = 0$ is primarily a result of specifying $G'(\omega) = 1$. In a real oscillator, the net gain is always slightly below unity so that a constant power can be maintained in the presence of noise injection.

Although many aspects of (3) are intuitively pleasing (such as its dependence on the ratio of noise to signal), the assumption of time-invariance ultimately does not hold for a real oscillator [3], [4]. As we will see in Section III, the timing (phase) of a noise event relative to the signal determines how the added noise power is split between amplitude and phase. In (1), we have implicitly assumed *every* instance of noise injection to have a fixed phase relative to the signal. As a result, the distinction between noise and a deterministic signal becomes lost. This picture violates our understanding of noise as a random process.

In Section III, we present a theory of phase noise that consistently resolves these issues. Our proposed model is applicable to any sinusoidal oscillator that can be represented in the configuration of Fig. 1. This encompasses a broad range of oscillators operating in both electrical and optical domains. We will show that these oscillators are all united by a common technique of analyzing noise in the oscillator's basis. The concept of a basis is fundamental to every physical system and thus explains the widespread applicability of our phase-noise model.

III. Phase-Noise Theory

A. Vector-Based Approach to Phase Noise

We begin by considering the oscillator electric field $E(t)$ represented as a phasor in the complex plane (Fig. 2) [9]. Its initial magnitude is normalized such that $E_0^2 = P_0$, where P_0 is the intracavity power of the signal. The oscillator's phase starts at an arbitrary angle ϕ with respect to the real axis. The addition of a noise event, having magnitude E_n such that $E_n^2 = P_n$ and relative phase θ_i, results in perturbation of both the amplitude and phase of the original oscillating field. As the phase of

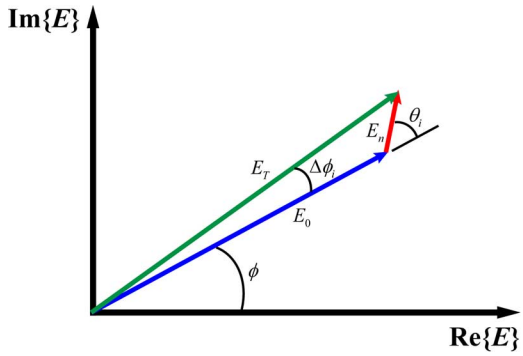

Fig. 2. Vector-based description of an oscillator's field under noise perturbation.

the noise event is random relative to that of the field, θ_i is uniformly distributed between 0 and 2π. The amplitude of the total signal vector (E_T) is given by $E_T^2 = P_0 + \Delta P_i$ where ΔP_i is defined as the change in oscillation power induced by a noise event having relative phase θ_i. From Fig. 2, we can calculate the phase perturbation $\Delta\phi_i$ to be

$$\Delta\phi_i = E_n \frac{\sin(\theta_i)}{E_0} \tag{4}$$

where we have approximated $E_T \approx E_0$ and $\sin(\Delta\phi_i) \approx \Delta\phi_i$. The approximations state that the amplitude and phase shift induced by *a single* noise event results in only small perturbations of the oscillator's total amplitude and phase. This statement is intuitive and does not contradict the unbounded divergence in the variance of the total accumulated phase [6]. Using similar techniques, one can also formulate an expression for ΔP_i as

$$\Delta P_i = P_n + 2\sqrt{P_0 P_n}\cos(\theta_i). \tag{5}$$

Equations (4) and (5) describe the time-varying interaction of signal and noise [3], [4]. If the noise is in-phase with the oscillation field $(\theta_i = 0)$, the noise appears only in the amplitude of the signal. If the noise is out-of-phase with the signal $(\theta_i = \pi/2)$, the noise primarily appears as a phase shift. Note that the first term on the right-hand side of (5) corresponds to the mean perturbation of the signal power (averaged over all θ_i) due to a single noise event. When also averaged over the strength of a noise event, this corresponds for a laser to the addition of one noise photon per optical mode [9]. For a general oscillator, P_n represents the noise power coupled into a single mode of the oscillator due to a single noise event. The fact that the axes that govern pure phase shift and pure amplitude shift are oblique and not orthogonal has previously been shown in [25].

Using the Wiener–Khinchin theorem, we proceed to calculate the phase-noise spectrum through the autocorrelation of the oscillating field (see the Appendix)

$$\langle E(t)^* E(t+\tau)\rangle \approx E_0^2 e^{j2\pi f_0 \tau} e^{-\langle\Delta\phi^2\rangle/2}. \tag{6}$$

In (6), f_0 is the oscillation frequency, τ is the time delay over which noise events are observed, and $\langle\Delta\phi^2\rangle$ is the second moment of the phase shift incurred over τ. As the phase shifts have zero mean, $\langle\Delta\phi^2\rangle$ is also the variance of the total phase shift. Since the oscillating power is stabilized around its mean, we can use (4) to define $\Delta\phi$ induced by M noise events through

$$\Delta\phi = \sum_{i=1}^{M} E_n \frac{\sin(\theta_i)}{E_0}. \tag{7}$$

Since each noise event is independent, the variance in phase shift can be shown to be

$$\langle\Delta\phi^2\rangle = \frac{\bar{P}_n}{2P_0} M \tag{8}$$

where $\bar{P}_n = \langle P_n\rangle$ is the average strength of a noise event. The factor of 1/2 in (8) is due to equipartitioning of the noise such that half of the noise power is used for driving phase fluctuations [10].

As a starting point, one could attempt to find E_n, P_n through the continuous spectrum of white noise. However, in doing so, one quickly finds that it becomes necessary to vectorially add noise to the oscillating field (Fig. 2), even when their individual frequencies are different. This is resolved through the realization that the continuum representation of noise outside the oscillator becomes inappropriate for describing noise within the confines of the oscillator boundaries. The noise must instead be distributed into the individual modes of the resonant system, which together form the basis of the oscillator. The average magnitude of the noise event $\bar{P}_n$ is thereby found by determining the amount of noise coupled into the oscillating mode. For the case of lasers, quantum theory establishes the average magnitude of a spontaneous emission event to be the equivalent of one noise photon per cavity mode [9], [10], [26]. The corresponding rate of spontaneous photon emission into the cavity mode per unit volume is denoted as R'_{sp} [9], [10]. To progress further in our development, we require a similar fundamental relation, but for the case of a general electromagnetic oscillator. In their laser analysis, the authors of [10] treat R'_{sp} by distributing the total spontaneous emission among the modes of the optical cavity. For the case of a white-noise spectrum, the noise is equally coupled into all the modes of the cavity. As the properties of noise are identical in electromagnetic oscillators, one expects this approach to be applicable outside the description of a laser.

At this point, it is useful to make a few comments regarding application of this formalism to a general theory of oscillator phase noise. First, the modes of a general cavity are 3-D in nature and are associated with various polarizations. Therefore, one must count the number of modes in all orthogonal directions and polarization states [10], [14], [17], [18]. For our purposes, we consider a linear cavity supporting a single polarization, both for simplicity and for comparison to our measured results for electrical oscillators. Note that although our description above implicitly assumes a Fabry–Perot resonator, the developed phase-noise theory can be applied to any oscillator configuration. The concept of a mode is general to any three-dimensionally confined structure, which we will designate by the term "cavity." In Section III-B, we will measure electrical oscillators based on ring cavity geometries (i.e., microwave components connected in a closed loop). The ring geometry can be obtained from a Fabry–Perot by unfolding the Fabry–Perot at its

reflection point. The electronic amplifier used in our oscillator only operates from 2 to 4 GHz, and thus only couples noise to the fundamental TEM mode of a coaxial line. If necessary, one can readily extend our approach to cavities of higher dimensionality and number of polarization states. Second, the various noise sources considered are white only up to a certain cutoff frequency. In cases where the spectral width of the noise only encompasses a few cavity modes, the noise is approximately partitioned into only those modes. This is analogous to the concept of a thresholdless laser where all of the spontaneous emission is consumed by a single mode of the cavity [15], [16], [19], [20]. Third, as gain is required to achieve oscillation, it is unphysical to have an oscillator where the amplifier noise and the oscillating cavity modes do not overlap. In systems where this overlap is small, both the gain and emission of noise become inhibited [27].

For an oscillator supporting a single transverse mode having a single polarization state over the frequency range where noise is generated, the noise power is only distributed into the longitudinal modes of the cavity. When the cavity is large such that the noise spectrum encompasses many longitudinal modes, one can compute the noise power per mode ($\bar{P}_n$) as

$$\bar{P}_n = \frac{N_{\rm psd}}{T} \tag{9}$$

where $N_{\rm psd}$ is the power spectral density of the white-noise perturbation and T is the total round-trip time delay of the cavity. Equation (9) is derived by integrating the white noise over a span Δf around the oscillating mode and subsequently dividing the result by the number of modes contained in Δf. This equation is intuitive as a larger T results in a larger density of longitudinal modes and thus reduced noise power coupled into each mode.

For white noise, the occurrence of M noise events in (8) corresponds to an average rate of noise injection ($R_{\rm inj}$) multiplied by an average observation time ($|\tau|$) [9]. We can combine all the noise sources encountered during a cavity round-trip through vector addition and treat the result as a single noise source acting on the signal of Fig. 2. The composite continues to satisfy (4) even if the total amplitude and phase shift are no longer small compared to that of the oscillating field (see the Appendix). The physics of the interaction are still governed by the phase and amplitude shifts of each individual noise event. Furthermore, as there is no distinction from one phase angle to the next, there can be no preference in direction of the resultant noise vector. The composite collection of noise thus obeys (6) and (7) with $\theta_{i,\rm tot}$ uniformly distributed between 0 and 2π. The total power ($\bar{P}_{n,\rm tot}$) of the combined noise is

$$\bar{P}_{n,\rm tot} = \frac{N_{\rm psd,tot}}{T} \tag{10}$$

representing the addition in average power for each of the individual sources. $N_{\rm psd,tot}$ is the power spectral density of the combined noise source that is injected once every cavity round-trip. The corresponding rate of injection is therefore $R_{inj,\rm tot} = 1/T$.

Incorporating the results of our previous discussion with (8) and (10), we find

$$\langle \Delta\phi^2 \rangle = \frac{N_{\rm psd,tot}}{2P_0T^2}|\tau|. \tag{11}$$

Thus, the variance of the phase shift is linearly proportional to the observation time of noise events. This diffusion in phase is analogous to the random movement of particles governed by Brownian motion. Substituting (11) into (6) and taking the Fourier transform, we find

$$S(f) = P_0\frac{1}{\pi}\frac{0.5\Delta f_{3\ \rm dB}}{(f-f_0)^2 + (0.5\Delta f_{3\ \rm dB})^2} \tag{12}$$

where

$$\Delta f_{3\ \rm dB} = \frac{N_{\rm psd,tot}}{4\pi P_0 T^2}. \tag{13}$$

Equation (13) is the main result of this analysis. It reveals that the oscillator full-width-at-half-power linewidth ($\Delta f_{3\ \rm dB}$) is primarily dependent on the noise-to-signal ratio. To achieve low phase-noise, the perturbation should be made small in comparison to the signal so that each noise event only weakly disturbs the oscillator's phase (Fig. 2). Furthermore, the round-trip time delay T should be made large so that the noise partitioned into each mode and its associated rate of injection decreases relative to the oscillating power. Dividing (12) by P_0, the corresponding normalized phase-noise spectrum is given by

$$L(f) = \frac{1}{\pi}\frac{0.5\Delta f_{3\ \rm dB}}{(f-f_0)^2 + (0.5\Delta f_{3\ \rm dB})^2}. \tag{14}$$

The form of (14) is similar to that of Leeson's empirical equation for an oscillator perturbed by white noise [1]. At frequencies much larger than the linewidth ($f \gg \Delta f_{3\ \rm dB}$), the phase-noise spectrum decays at 20 dB/decade scaled by the noise-to-signal ratio. However, unlike LTI models of phase noise, the derivation of (14) makes clear the random nature of noise in its interaction with the oscillating field.

B. Unification With Laser Theory

In this section, we unify the concepts of oscillator phase noise across the electrical and optical domains. At optical frequencies, it is well established that the laser phase-noise follows a Lorentzian similar to (14), but with a modified linewidth appropriate to the description of a laser [9], [10]. Our aim here is to show that the framework offered by (13) and (14) is consistent with conventional models of laser linewidth.

We begin by decomposing (13) into its fundamental components: a ratio of the noise to the signal multiplied by the rate at which noise is injected. Our previous analysis identifies the noise term as the total round-trip noise that couples into a single mode (i.e., the oscillating mode) of the cavity ($N_{\rm psd,tot}/T$). On the other hand, the signal term represents the total power accumulated in the oscillating mode (P_0). As we have grouped the noise into a combined total that is added every cavity round-trip,

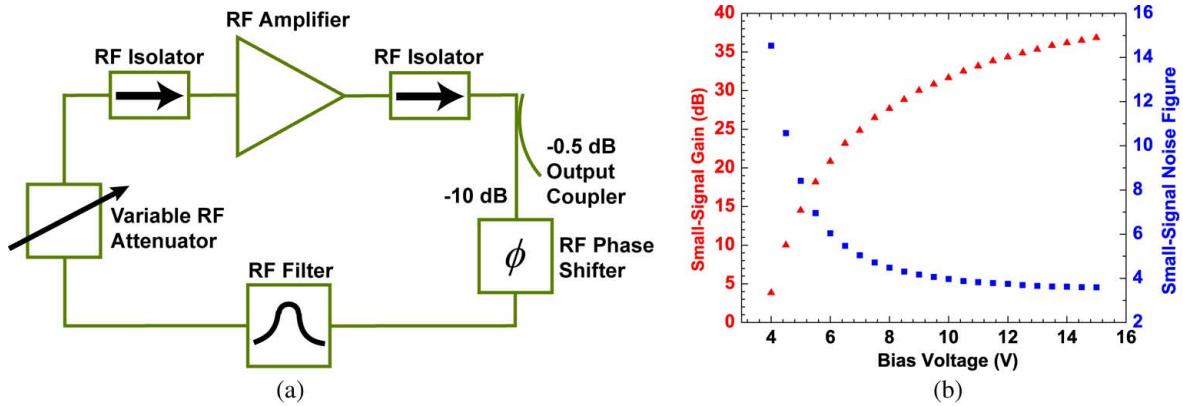

Fig. 3. (a) Schematic of the ring oscillator circuit and (b) measured gain and NF of the RF amplifier as a function of bias voltage. The system delay is defined by various configurations of RF filters controlling the net group delay per cavity round-trip. The RF signal is coupled out prior to filtering allowing for direct measurement of the noise added in each round-trip.

the rate of noise injection is given by the inverse of the round-trip delay $(1/T)$.

These terms all have analogous, albeit slightly modified, interpretations in laser physics. For example, the signal power is described through N_p, which is defined as the photon density contained within the oscillating mode. Although not directly in power units, the photon density and the oscillating power are related through the group velocity of the medium along with several other factors [9], [10]. These factors will be cancelled by defining the noise in the numerator through photon density units. In these units, the total noise injected into the oscillating mode over a cavity round-trip is given by $VR'_{sp}T/V_p$. Here, V is the active volume and V_p is the total photon volume (active + passive) including the effects of refractive index. Their ratio $(\Gamma = V/V_p)$ is termed the confinement factor and represents the overlap of the optical mode with the active material. R'_{sp} is the rate of spontaneous photon emission (per unit active volume [10]) injected into a single mode. When multiplied by the active volume and the time period of a cavity round-trip, $VR'_{sp}T$ represents the total noise injected into an oscillator mode per round-trip. To convert to photon density units, the noise is divided by the photon volume. Note that since the total noise was defined over a cavity round-trip, the corresponding rate of noise injection remains at $1/T$.

Inserting these terms into (13), the laser linewidth is found to be

$$\Delta f_{3\text{ dB,optical}} = \frac{\Gamma R'_{sp}}{4\pi N_p} \tag{15}$$

which exactly matches the expressions derived from conventional laser theory [9], [10]. This equivalence unifies the understanding of phase noise for both electrical and optical oscillators.

IV. Experimental Results

A. Comparisons to Measurement: Electrical RF Oscillator

To validate our theory, we first compare (13) and (14) to the measured phase noise of an electrical oscillator whose configuration is provided in Fig. 3(a). The ring cavity oscillates at a frequency of 2.5 GHz using gain supplied by an Avantek 2–4-GHz AM-4080M RF amplifier ($G = 25$ dB at 6.9 V, small-signal noise figure (NF) $\text{NF}_{\text{ss}} = 5.1$ dB). The passive components of the cavity consist of isolators at the RF amplifier input and output, an RF phase shifter for tuning the oscillation frequency, an RF filter for defining the center frequency, and a variable RF attenuator for control of intracavity loss. An output coupler is used to couple out most (90%) of the intracavity power, while the remainder (-10 dB) of the power is reused within the cavity to enable oscillation. Three different combinations of RF filters and delay were tested during our oscillator measurements: 1) tunable RF filter (halfwidth $(\text{HW}) = 75$ MHz at 2.5 GHz); 2) tunable RF filter $(\text{HW} = 75$ MHz) with 5.5 m additional delay; and 3) fixed RF filter $(\text{HW} = 2.9$ MHz). For each configuration, the center frequency was 2.5 GHz.

Fig. 4 shows the oscillator's phase-noise and amplitude-noise spectra for the three different RF filter/delay configurations as measured by a commercial Agilent E5052B signal-source analyzer (SSA). These measurements were conducted at RF output powers of -10.0 and -6.5 dBm and include $\sim$4.4 dB of loss between the RF coupler output and the SSA (due to cabling and a variable attenuator for output control). The oscillator was operated at low powers in order to prevent flicker noise from dominating over white noise at low offset frequencies. The oscillator output power was controlled by varying the bias voltage of the RF amplifier (between 6.7–6.9 V). In all of our measurements, the intracavity variable attenuator was adjusted so that the loss within the oscillator loop was kept constant. The primary effect of the different filters/delay configurations then is to introduce different time delays to the oscillating mode as a result of the group delay induced by the filter resonance. The phase noise decreases at 20 dB/decade as predicted for Lorentzian broadening due to white noise injection [see (14)]. It is clear from Fig. 4 that the measured phase noise is greatly influenced by the RF filter/delay combination used. The corresponding amplitude noise is seen to be much lower in comparison. Note that 40 MHz is the maximum offset frequency of the SSA amplitude-noise measurement. The origin of the peaks near $\sim$400 kHz in Fig. 4(b) and (d) is currently unknown. However, the side modes of the oscillator can clearly be seen above 20 MHz in all of the spectra. As expected, the side-mode spacing decreases for an increase in round-trip delay. With the fixed filter, the

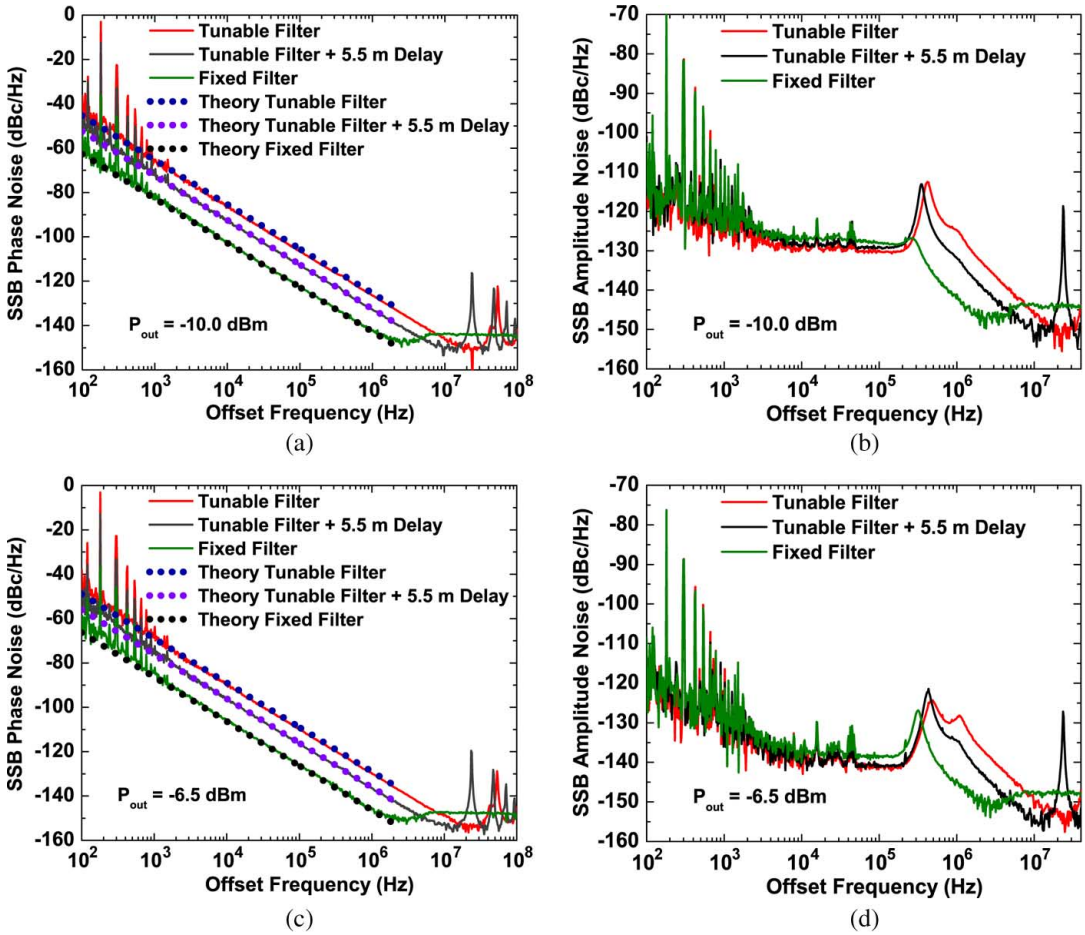

Fig. 4. Measured RF oscillator phase-noise and amplitude-noise. (a) Measured phase-noise spectra and theory at −10.0-dBm RF power. (b) Amplitude-noise spectra at −10.0-dBm RF power. (c) Measured phase-noise spectra and theory at −6.5-dBm RF power. (d) Amplitude-noise spectra at −6.5-dBm RF power. The RF oscillator of Fig. 3 was tested with three filter configurations including: 1) a tunable filter; 2) a tunable filter +5.5-m delay; and 3) a fixed filter. The various filter configurations change the effective round-trip delay through the associated resonances of the filters.

filter bandwidth is narrow enough to reject all of the cavity side modes. In this case, the side-mode spacing was determined from the frequency translation of the oscillating mode corresponding to a 2π shift in cavity phase. The frequencies of the side modes were measured to be 53.5 MHz for the tunable filter, 23.6 MHz for the tunable filter +5.5 m delay, and 7.3 MHz for the fixed filter.

The phase-noise spectrum can be calculated from (13) and (14) once the oscillation power, injected noise power, and round-trip time delay are known. The round-trip delay (T) is directly found from the inverse of the measured side-mode frequency spacing. Usually, knowledge of the amplifier's NF is required to estimate the noise added in a single round-trip. However, in our case, $N_{\mathrm{psd,tot}}$ can be directly measured from the noise beyond 10-MHz offset for the case of the fixed filter (Fig. 4). Since we have coupled out the power before filtering [see Fig. 3(a)], the noise power at large offset frequencies is exactly the white-noise power injected every cavity round-trip. The narrow filter bandwidth prevents the accumulation of noise at these frequencies. Equipartition can be verified as the injected noise is equal in both the measured amplitude- and phase-noise plots. The sum of both contributions yields a total noise $(N_{\mathrm{psd,tot}})$ of −141.0 dBc/Hz at −10.0 dBm and −144.6 dBc/Hz at −6.5 dBm referenced to the carrier. The additive noise is invariant with signal power causing the relative ratio to decrease with increasing power. Note that our theory does not apply for multiplicative noise (which scales proportionally to signal power) resulting from the upconversion of near-dc flicker noise. In principle, the measured noise and signal should be traced back to the input of the amplifier stage. However, as the ratio of noise to signal is invariant under attenuation, (13) can be evaluated directly from our measurements of the total noise (relative to carrier). Furthermore, since the same operating conditions (intracavity loss, RF power, and RF amplifier bias) were used for all three filter configurations, the total noise is constant at each RF power level. Note that the injected noise cannot otherwise be measured in the tunable filter configurations since the side modes are not completely rejected in Fig. 4. Using (13) and (14) and the directly measured parameters (i.e., no fitting parameters), the oscillator phase noise was calculated for each of the cases and plotted (dotted line) against the measurement. The excellent agreement between theory and experiment verifies the inverse dependence of phase noise on the square of the round-trip time. The dependence of phase noise on the inverse of signal power can also be observed in Fig. 4, but is more clearly illustrated in Fig. 5.

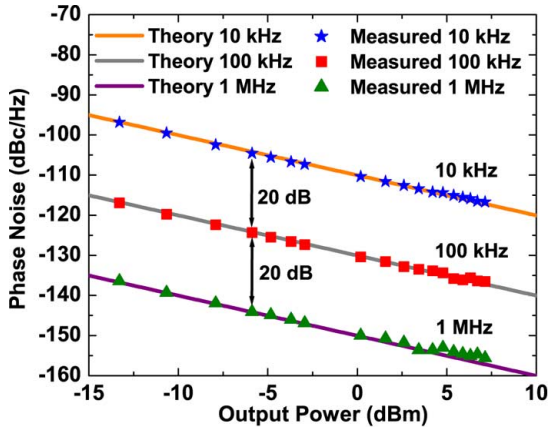

Fig. 5. Measured and theoretical power dependence of oscillator phase noise.

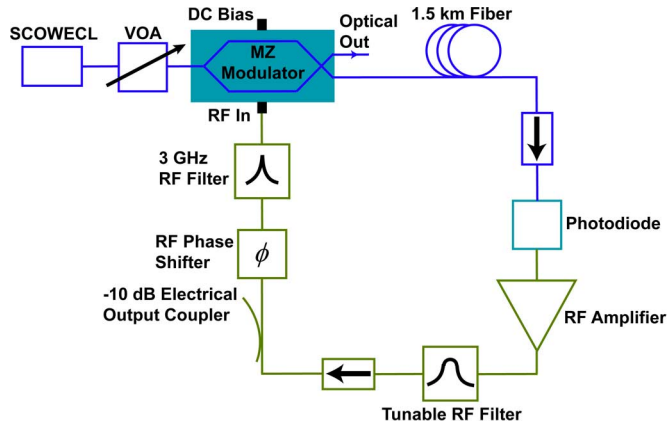

Fig. 6. Configuration of an OEO operating at 3.0 GHz. MWP gain is achieved by the high-power low-noise SCOWECL, MZ modulator, and photodiode.

For the measurements of Fig. 5, we use the same oscillator configuration as that of Fig. 3(a), but with an RF filter consisting of the cascade between the tunable and fixed filters. The side-mode spacing decreases to 6.8 MHz reflecting the additional phase delay through the filter cascades. The output power was varied between -13.3 and 7.3 dBm through control of the RF amplifier bias voltage. Note that these measurements include $\sim$4.4 dB of loss between oscillator output and the SSA. In Fig. 5, the measured phase noise is plotted against RF power for offset frequencies of 10 kHz, 100 kHz, and 1 MHz. Using the methods described previously, the phase noise was also calculated at these frequencies for operation at -13.3 dBm. The theory is then extrapolated to other RF powers using a $1/P_0$ dependence. This allows the comparison of experiment and theory over the entire range of oscillator power. As can be observed in Fig. 5, the agreement is excellent between the two. The inverse dependence of phase noise on signal power can be clearly seen with 20-dB separation in phase noise between each decade of offset frequency.

It is also possible to directly evaluate the phase noise using the NF of the RF amplifier along with knowledge of the input power. Typically, the measured small-signal NF ($\mathrm{NF_{ss}}$) of the RF amplifier is dependent on the bias applied. For the measurement range of Fig. 5, $\mathrm{NF_{ss}}$ varies from 4.7 dB at 7.5-V bias ($P_{\mathrm{out}} = -13.3$ dBm) to 3.6 dB at 13.8-V bias ($P_{\mathrm{out}} = 7.3$ dBm) [see Fig. 3(b)]. However, the NF required for evaluating the phase noise of (13) and (14) is that under the large-signal operating conditions of the oscillator. Under these conditions, we find the NF to be approximately clamped at its value during the onset of oscillation, independent of applied bias. This is analogous to the clamping of a laser's spontaneous emission above threshold [10]. The large-signal NF extracted from all the cases tested in Fig. 5 is 5.1 dB. This agrees well with $\mathrm{NF_{ss}} = 4.8$ dB independently measured at the oscillation threshold voltage of 7.4 V. Note, for the cases of Fig. 4, the extracted NF was 5.8 dB, and the corresponding $\mathrm{NF_{ss}}$ was independently measured to be 5.5 dB at an oscillation threshold of 6.4 V.

B. Comparisons to Measurement: OEO Limited by White Noise

Since many electromagnetic oscillators can be represented in the form of an equivalent amplifier in a resonant cavity (Fig. 1), the theory of (13) and (14) can in principle be applied beyond the simple ring oscillators of the previous section. In this section, we apply the developed phase-noise theory to a hybrid OEO [2], [22]–[24]. The OEO (Fig. 6) comprises both electrical and optical cavity elements, and amplification is achieved via microwave-photonic (MWP) gain [28].

Its optical loop consists of a high-power low-noise slab-coupled optical waveguide external cavity laser (SCOWECL) [29], [30] ($P = 250$ mW at 3-A bias), a variable optical attenuator (VOA), a Mach–Zehnder (MZ) modulator (BW $= 15$ GHz, $V_\pi = 3.1$ V at 3 GHz), a 1.5-km-long spool of single-mode optical fiber, an optical isolator, and a commercial photodiode ($\Re = 0.8$ A/W, BW $= 12$ GHz). In the electrical path, the photodiode output is amplified by a low flicker-noise AML26PNB2001 2–6-GHz RF amplifier ($G = 23.4$ dB, $\mathrm{NF_{ss}} = 5.7$ dB) before passing through a tunable RF filter ($f_{\mathrm{center}} = 3.0$ GHz, HW $= 95$ MHz at 3.0 GHz), an electrical isolator, an RF phase shifter, and a fixed 3.0-GHz RF filter (HW $= 1.2$ MHz). The opto-electronic loop is closed by feeding the electrical signal back as the input to the optical modulator. The cascade consisting of the SCOWECL, modulator, and photodiode provides heterodyne gain due to beat-note generation from modulator RF-in to photodiode RF-out. RF amplification was used as the MWP gain was not sufficient to overcome the losses of the system.

Oscillation begins from the amplification of noise incident on the modulator RF input port. The oscillation signal is accessed through a -10-dB RF coupler located after the RF isolator. As was done for the electrical ring oscillator case, the signal is coupled out prior to the 3-GHz RF filter (HW $= 1.2$ MHz) for measurement of the noise added in each cavity round-trip. However, as we found the operation and measurement of the OEO to be sensitive to out-of-band noise, we included a second tunable filter (HW $= 95$ MHz) for stabilization of the OEO. The difference in filter bandwidths allows for a reasonably broad range where the injected noise may be measured. The SCOWECL was operated at 3-A bias for our measurements, while its output power was controlled using the VOA.

The OEO operates by modulation of the optical carrier with a coherent RF envelope. This RF envelope is photodetected, filtered, and reused as the input to the modulator. We may represent the cascade of the SCOWECL, MZ modulator, fiber

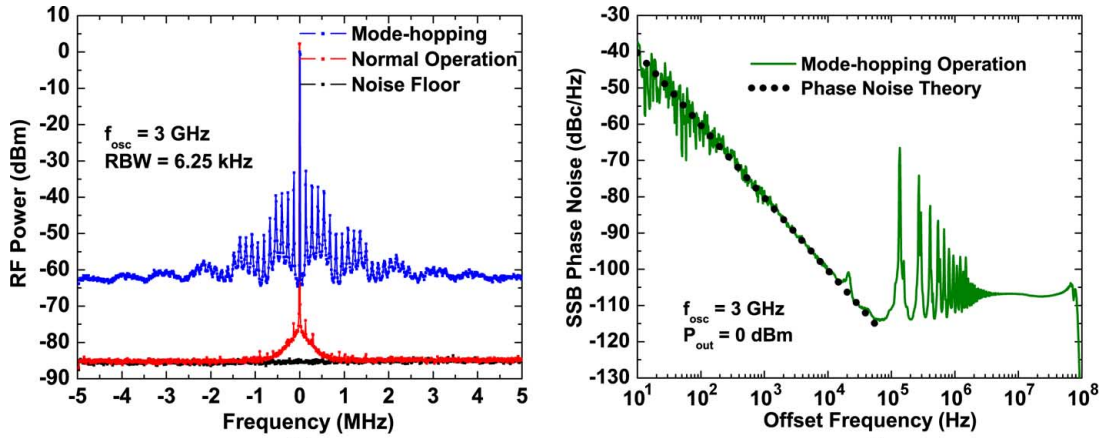

Fig. 7. RF spectrum and phase-noise of an OEO. (a) RF spectrum showing OEO performance when the laser is operated under mode-hopping conditions. The spectrum for normal operation is also provided. (b) Phase noise of the OEO operated under laser mode-hopping conditions. The white injected noise dominates, resulting in a Lorentzian phase-noise spectrum.

delay, photodiode, and RF amplifier as an equivalent amplifier with an effective delay corresponding to 1.5 km of optical fiber (Fig. 1). This equivalent amplifier is placed within the RF loop of the OEO and filtered each round-trip. The addition of incoherent noise (thermal noise, shot noise, laser relative intensity noise (RIN), and nonlinear fiber noise) causes perturbations of random phase to the coherent RF envelope [23]. This results in spectral broadening of the oscillation signal. It is straightforward to show that the noise is only partitioned into the longitudinal modes of an OEO. Since the MZ modulator was designed for a single polarization, only that polarization within the optical loop may receive gain, and thus noise injection from the MWP link. The use of single-mode fiber also prevents the excitation of higher order transverse modes over the gain bandwidth of the laser. In the RF loop, the bandwidth limitations of the modulator and photodiode ($\sim$10 GHz) prevent operation outside of the fundamental TEM mode of the coaxial line. Thus, the combined OEO modes are only described by the longitudinal indices of the cavity.

The modulation and photodetection processes in an OEO result in the mixing of noise near baseband with noise at microwave frequencies. Therefore, the laser RIN at low frequencies is upconverted into the frequency range of oscillation [23]. Typically the RIN at low frequencies dominates, which along with nonlinear fiber noise, result in the prevalence of colored noise in an OEO. However, we find that when the SCOWECL is operating under typically undesired mode-hopping conditions, the total noise is white and dominated by the high-frequency RIN of the laser. This can be verified in the RF spectrum of the 3-GHz OEO in Fig. 7(a).

Fig. 7(b) shows the measured OEO phase noise when the SCOWECL is operated in the mode-hopping regime. The operating photocurrent was 5.9 mA, and the output RF power (with cable losses) is $\sim$0 dBm. The spectrum falls at 20 dB/decade, characteristic of a Lorentzian. The side-mode frequency spacing ($\sim 1/T$) is 135 kHz, corresponding to a fiber delay of 1.5 km. The injected round-trip noise can be found from the spectrum at frequencies near 10-MHz offset. The total noise ($N_{\mathrm{psd,tot}}$) resulting from both amplitude and phase contributions is -104 dBc/Hz relative to the carrier. Note that the sharp cutoff in phase noise near 90 MHz is due to the stopband of the tunable filter. Using these measured parameters in (13) and (14), the theoretical OEO phase noise was computed and graphed against the measurement results in Fig. 7(b). The agreement is once again excellent over the frequency range tested *with no fitting parameters*. We see that the phase noise of the OEO is comparable to that of the fixed-filter RF oscillator in Fig. 4(a) despite having a 37-dB lower signal-to-noise ratio (SNR). The degradation in phase noise through the SNR is balanced by the improvement in phase noise gained through using a longer round-trip delay (54$\times$ compared to that of the fixed-filter oscillator cavity). This example illustrates the power of using delay to reduce phase noise. However, the lowest phase noise is achieved when both SNR and delay are maximized.

V. Discussion

Before concluding, we wish to address two potential points of confusion in our analysis. First, as the derivations of (13) and (14) are based on noise perturbation, it is interesting to discuss the distinction between an oscillator and an amplifier. In an amplifier, one does not expect to see Lorentzian broadening of the line shape after signal amplification. Yet, the intuition offered by Fig. 2 does not appear to differentiate between the two systems. The key difference is that the modes of an amplifier form a continuum as there is no associated resonant cavity. A one-to-one mapping exists between the amplifier continuum and noise, and thus the noise becomes directly added to the spectrum at all frequencies. This direct summing of noise power with the oscillator spectrum is the basis for the concept of NF in both electrical [31] and optical amplifiers [32].

Second, although the validity of our phase-noise model was only specifically justified for the cases of electrical and optical oscillators, the scope of our approach is expected to be even more far reaching. As long as the oscillator can be represented as an equivalent amplifier in a resonant configuration (Fig. 1), one needs only to partition the noise among the independent modes of the system. The addition of incoherent noise to a coherent oscillation signal results in phase diffusion and spectral broadening. With the appropriate definition of system parameters, our

theory should also prove applicable to mechanical oscillators as well as oscillators of other variety.

VI. Conclusion

We have provided a general approach to the solution of oscillator phase noise when the oscillating field is sinusoidal and perturbed by additive white noise. Our theory is intuitive and based on the partitioning of noise into the modes of the cavity. This partitioning is fundamental to any physical system whose basis becomes defined by the system boundaries. We have also unified our phase-noise theory with interpretations of linewidth derived from laser physics. For purposes of verification, we have measured the phase noise of RF oscillators with both round-trip delay and intracavity power as free parameters. We have also constructed a hybrid OEO whose operation is based on entirely different principles. In both cases, excellent agreement is found between calculated phase-noise spectra and those measured experimentally. The intuition offered by our approach should prove beneficial for future extension to cases of $1/f^{\alpha}$ noise.

Appendix

A. Derivation of the Phase-Noise Spectrum

Starting from the electric field $E(t)$ of the oscillator,

$$E(t) = \sqrt{2}\left[E_0 + \Delta E(t)\right]\cos\left(\omega_0 t + \phi(t)\right) \tag{A.1}$$

we can calculate the spectrum through application of the Wiener–Khinchin theorem [33]

$$S(\omega) = \mathrm{FT}\left\langle E(t)^* E(t+\tau)\right\rangle. \tag{A.2}$$

Here, E_0 is the initial field amplitude, $\Delta E(t)$ is the time-dependent amplitude shift, ω_0 is the oscillation frequency, $\phi(t)$ is the time-dependent oscillator phase, τ is the time delay of observation, and FT denotes the Fourier transform operation. Note that $E(t)$ in (A.1) is normalized so that the average power is E_0^2. The autocorrelation is evaluated directly

$$\begin{aligned}
&\left\langle E(t)^* E(t+\tau)\right\rangle \\
&\quad= \left\langle \frac{\left[E_0 + \Delta E(t)\right]\left[E_0 + \Delta E(t+\tau)\right]}{2} \right. \\
&\qquad\left. \times\, e^{j(\omega_0\tau + \phi(t+\tau) - \phi(t))} \right\rangle \\
&\qquad+ \left\langle \frac{\left[E_0 + \Delta E(t)\right]\left[E_0 + \Delta E(t+\tau)\right]}{2} \right. \\
&\qquad\left. \times\, e^{-j(2\omega_0 t + \omega_0\tau + \phi(t+\tau) + \phi(t))} \right\rangle \\
&\qquad+ \left\langle \frac{\left[E_0 + \Delta E(t)\right]\left[E_0 + \Delta E(t+\tau)\right]}{2} \right. \\
&\qquad\left. \times\, e^{j(2\omega_0 t + \omega_0\tau + \phi(t+\tau) + \phi(t))} \right\rangle \\
&\qquad+ \left\langle \frac{\left[E_0 + \Delta E(t)\right]\left[E_0 + \Delta E(t+\tau)\right]}{2} \right. \\
&\qquad\left. \times\, e^{-j(\omega_0\tau + \phi(t+\tau) - \phi(t))} \right\rangle.
\end{aligned} \tag{A.3}$$

Since the second and third terms on the right-hand side average to zero, the autocorrelation evaluates to

$$\begin{aligned}
&\left\langle E(t)^* E(t+\tau)\right\rangle \\
&\quad= \left\langle \frac{1}{2}\left[E_0^2 + E_0\Delta E(t+\tau) + E_0\Delta E(t)\right.\right. \\
&\qquad\left.\left. +\Delta E(t)\Delta E(t+\tau)\right]\left(e^{j(\omega_0\tau+\Delta\phi)} + e^{-j(\omega_0\tau+\Delta\phi)}\right)\right\rangle.
\end{aligned} \tag{A.4}$$

Equation (A.4) introduces the variable $\Delta\phi = \phi(t+\tau) - \phi(t)$ corresponding to the total phase shift occurring over an observation time τ. In general, the correlations between amplitude and phase in (A.4) are nonzero [5] as a single noise event generates both amplitude and phase fluctuations. However, the amplitude noise is usually greatly suppressed relative to phase noise due to the oscillator's intrinsic negative feedback and also to various amplitude-limiting elements in the cavity (e.g., the amplifier). The oscillator's autocorrelation is therefore approximately due to phase fluctuations and evaluates to

$$\left\langle E(t)^* E(t+\tau)\right\rangle = \left\langle \frac{E_0^2}{2}\left(e^{j(\omega_0\tau+\Delta\phi)} + e^{-j(\omega_0\tau+\Delta\phi)}\right)\right\rangle. \tag{A.5}$$

It is clear from (A.5) that the individual terms on the right-hand side represent the positive and negative frequencies of the corresponding spectrum. We can thus represent the autocorrelation through a phasor with only positive frequencies explicit.

As the oscillator phase is defined through a series of many noise events, it is reasonable to expect from the central limit theorem that the phase distribution follows a Gaussian. Starting from the Fokker–Planck equation, [6] proves this to be exactly true for infinite observation time. Reference [6] also shows that only the cumulants of first and second order survive in $\Delta\phi$, and therefore the total phase shift is also Gaussian distributed. Evaluation of the expectation value then requires only the integration of (A.5) multiplied by a Gaussian probability density

$$\begin{aligned}
\left\langle E(t)^* E(t+\tau)\right\rangle &= E_0^2\left\langle e^{j(\omega_0\tau+\Delta\phi)}\right\rangle \\
&= \frac{E_0^2 e^{j\omega_0\tau}}{\sqrt{2\pi\sigma^2}}\int_{-\infty}^{\infty} e^{j\Delta\phi} e^{-\frac{\Delta\phi^2}{2\sigma^2}}\, d\Delta\phi \\
&= E_0^2 e^{j2\pi f_0\tau} e^{-\langle\Delta\phi^2\rangle/2}.
\end{aligned} \tag{A.6}$$

In evaluating (A.6), we have used the fact that the average phase shift (first moment) is zero, and thus the variance in phase shift σ^2 is given by its second moment $\langle\Delta\phi^2\rangle$.

B. Vector Combination of Noise Sources

Here, we show that the vector of combined noise sources satisfies (4) for a single round-trip of the oscillator. We begin with the total phase shift $\Delta\phi_{\mathrm{RT}}$ due to M_{RT} noise events in a cavity round-trip. The contribution of noise over a round-trip yields a net phase shift

$$\Delta\phi_{\mathrm{RT}} = \sum_{i=1}^{M_{\mathrm{RT}}} E_n \frac{\sin\theta_i}{E_0}. \tag{B.1}$$

Here, E_n is the field amplitude of a noise event, E_0 is the field amplitude of the signal, and θ_i is the phase of the noise relative to the oscillating field. We can equivalently combine the noise events over the time of a round-trip into a combined noise vector $(E_{n,\mathrm{tot}})$ through

$$E_{n,\mathrm{tot}} = \sum_{i=1}^{M_{\mathrm{RT}}} E_n e^{j\theta_i} = \sqrt{\left(\sum_{i=1}^{M_{\mathrm{RT}}} E_n \cos\theta_i\right)^2 + \left(\sum_{i=1}^{M_{\mathrm{RT}}} E_n \sin\theta_i\right)^2} \times e^{j\tan^{-1}\left(\sum_{i=1}^{M_{\mathrm{RT}}} E_n \sin\theta_i / \sum_{i=1}^{M_{\mathrm{RT}}} E_n \cos\theta_i\right)}. \quad \text{(B.2)}$$

Applying (4), the combined phase shift $(\Delta\phi_{\mathrm{tot}})$ is

$$\Delta\phi_{\mathrm{tot}} = \frac{|E_{n,\mathrm{tot}}|}{E_0}\sin(\angle E_{n,\mathrm{tot}}) = \frac{\sum_{i=1}^{M_{\mathrm{RT}}} E_n \sin\theta_i}{E_0}. \quad \text{(B.3)}$$

The equivalence of (B.1) and (B.3) establishes the validity of representing the round-trip noise through a combined noise vector, even if the total amplitude and phase shift are no longer small compared to that of the oscillating field.

ACKNOWLEDGMENT

The authors would like to thank Prof. F. X. Kaertner, Massachusetts Institute of Technology (MIT), Cambridge, MA, USA, for valuable discussions and guidance.

REFERENCES

[1] D. B. Leeson, "A simple model of feedback oscillator noise spectrum," *Proc. IEEE*, vol. 54, no. 2, pp. 329–330, Feb. 1966.
[2] X. S. Yao and L. Maleki, "Optoelectronic microwave oscillator," *J. Opt. Soc. Amer. B, Opt. Phys.*, vol. 13, no. 8, pp. 1725–1735, Aug. 1996.
[3] A. Hajimiri and T. H. Lee, "A general theory of phase noise in electrical oscillators," *IEEE J. Solid-State Circuits*, vol. 33, no. 2, pp. 179–194, Feb. 1998.
[4] T. H. Lee and A. Hajimiri, "Oscillator phase noise: A tutorial," *IEEE J. Solid-state Circuits*, vol. 35, no. 3, pp. 326–336, Mar. 2000.
[5] F. X. Kaertner, "Analysis of white and $f^{-\alpha}$ noise in oscillators," *Int. J. Circuit Theory Appl.*, vol. 18, no. 5, pp. 485–519, Sep. 1990.
[6] A. Demir, A. Mehrotra, and J. Roychowdhury, "Phase noise in oscillators: A unifying theory and numerical methods for characterization," *IEEE Trans. Circuits Syst. I, Fundam. Theory Appl.*, vol. 47, no. 5, pp. 655–674, May 2000.
[7] A. L. Schawlow and C. H. Townes, "Infrared and optical masers," *Phys. Rev.*, vol. 112, no. 6, pp. 1940–1949, Dec. 1958.
[8] M. Lax, "Classical noise V: Noise in self-sustained oscillators," *Phys. Rev.*, vol. 160, no. 2, pp. 290–307, Aug. 1967.
[9] C. H. Henry, "Theory of the linewidth of semiconductor lasers," *IEEE J. Quantum Electron.*, vol. 18, no. 2, pp. 259–264, Feb. 1982.
[10] L. A. Coldren and S. W. Corzine, *Diode Lasers and Photonic Integrated Circuits*. New York, NY, USA: Wiley, 1995, pp. 140–187.
[11] P. W. Milonni and P. L. Knight, "Spontaneous emission between mirrors," *Opt. Commun.*, vol. 9, no. 2, pp. 119–122, Oct. 1973.
[12] H. H. França, T. W. Marshall, and E. Santos, "Spontaneous emission in confined space according to stochastic electrodynamics," *Phys. Rev. A, Gen. Phys.*, vol. 45, no. 9, pp. 6436–6442, May 1992.
[13] E. M. Purcell, "Spontaneous emission probabilities at radio frequencies," *Phys. Rev.*, vol. 69, p. 681, 1946.
[14] S. D. Brorson, H. Yokoyama, and E. P. Ippen, "Spontaneous emission rate alteration in optical waveguide structures," *IEEE J. Quantum Electron.*, vol. 26, no. 9, pp. 1492–1499, Sep. 1990.
[15] T. Baba, T. Hamano, F. Koyama, and K. Iga, "Spontaneous emission factor of a microcavity DBR surface-emitting laser," *IEEE J. Quantum Electron.*, vol. 27, no. 6, pp. 1347–1358, Jun. 1991.
[16] T. Baba, T. Hamano, F. Koyama, and K. Iga, "Spontaneous emission factor of a microcavity DBR surface-emitting laser (II)—Effects of electron quantum confinement," *IEEE J. Quantum Electron.*, vol. 28, no. 5, pp. 1310–1319, May 1992.
[17] K. Petermann, "Calculated spontaneous emission factor for double-heterostructure injection lasers with gain-induced waveguiding," *IEEE J. Quantum Electron.*, vol. QE-15, no. 7, pp. 566–570, Jul. 1979.
[18] Y. Yamamoto, S. Machida, and G. Björk, "Micro-cavity semiconductor laser with enhanced spontaneous emission," *Phys. Rev. A*, vol. 44, no. 1, pp. 657–668, Jul. 1991.
[19] F. De Martini and G. R. Jacobovitz, "Anomalous spontaneous-stimulated-decay phase transition and zero-threshold laser action in a microscopic cavity," *Phys. Rev. Lett.*, vol. 60, no. 17, pp. 1711–1714, Apr. 1988.
[20] H. Yokoyama *et al.*, "Controlling spontaneous emission and threshold-less laser oscillation with optical microcavities," *Opt. Quantum Electron.*, vol. 24, no. 2, pp. S245–S272, 1992.
[21] W. Loh, S. Yegnanarayanan, R. J. Ram, and P. W. Juodawlkis, "Unified theory of oscillator phase noise II: Flicker noise," *IEEE Trans. Microw. Theory Techn.*, to be published.
[22] L. Maleki, "Sources: The optoelectronic oscillator," *Nature Photon.*, vol. 5, pp. 728–730, Dec. 2011.
[23] W. Loh *et al.*, "Amplifier-free slab-coupled optical waveguide optoelectronic oscillator systems," *Opt. Exp.*, vol. 20, no. 17, pp. 19589–19598, Aug. 2012.
[24] W. Loh, S. Yegnanarayanan, R. J. Ram, and P. W. Juodawlkis, "Super-homogeneous saturation of microwave-photonic gain in optoelectronic oscillator systems," *IEEE Photon. J.*, vol. 4, no. 5, pp. 1256–1266, Oct. 2012.
[25] A. Demir and J. Roychowdhury, "On the validity of orthogonally decomposed perturbations in phase noise analysis," Bell Labs., Murray Hill, NJ, USA, Tech. Memo., 1997.
[26] A. E. Siegman, *Lasers*. Mill Valley, CA, USA: Univ. Sci. Books, 1986, pp. 497–505.
[27] E. Yablonovitch, "Inhibited spontaneous emission in solid-state physics and electronics," *Phys. Rev. Lett.*, vol. 58, no. 20, pp. 2059–2062, May 1987.
[28] C. H. Cox, III, *Analog Optical Links: Theory and Practice*. Cambridge, U.K.: Cambridge Univ. Press, 2004, ch. 3.
[29] W. Loh *et al.*, "Packaged, high-power, narrow-linewidth slab-coupled optical waveguide external cavity laser (SCOWECL)," *IEEE Photon. Technol. Lett.*, vol. 23, no. 14, pp. 974–976, Jul. 2011.
[30] P. W. Juodawlkis *et al.*, "High-power, low-noise 1.5 μm slab-coupled optical waveguide (SCOW) emitters: Physics, devices, and applications," *IEEE J. Sel. Top. Quantum Electron.*, vol. 17, no. 6, pp. 1698–1714, Nov. 2011.
[31] H. T. Friis, "Noise figure of radio receivers," *Proc. IRE*, vol. 32, no. 7, pp. 419–422, Jul. 1944.
[32] H. A. Haus, *Electromagnetic Noise and Quantum Optical Measurements*. Berlin, Germany: Springer, 2000, pp. 333–340.
[33] A. Khintchine, "Korrelationstheorie der stazionaren stochastischen Prozesse," *Math. Ann.*, vol. 109, pp. 604–615, 1934.

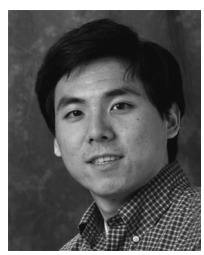

William Loh (S'10) received the B.S. degree in electrical engineering from The University of Michigan at Ann Arbor, Ann Arbor, MI, USA, in 2007, the M.S. degree in electrical engineering from the Massachusetts Institute of Technology (MIT), Cambridge, MA, USA, in 2009, and is currently working toward the Ph.D. degree in electrical engineering at MIT.

He is currently an active participant in the Integrated Photonics Initiative (IPI) collaboration between MIT and the MIT Lincoln Laboratory. His research interests include novel structures and schemes for semiconductor optical devices, MWP oscillators for synthesis of low-noise RF signals, physics of noise processes in oscillators and opto-electronic systems, and modeling of optical phenomena in photonic systems and devices.

Siva Yegnanarayanan (S'92–M'00) received the B.S. degree from the Indian Institute of Technology (IIT), Madras, India, the M.S. degree from the University of Maryland Baltimore County, Baltimore, MD, USA, and the Ph.D. degree from the University of California at Los Angeles, Los Angeles, CA, USA, all in electrical engineering.

From 1999 to 2000, he was a Staff Scientist with the Alcatel Corporate Research Center. In 2000, he joined Cognet Microsystems Inc. From 2001 to 2004, he was with the Intel Corporation. From 2004 to 2010, he was a Staff Scientist with the Photonics Research Group, Georgia Institute of Technology. In 2010, he joined the Electro-Optical Materials and Devices Group, Lincoln Laboratory, Massachusetts Institute of Technology (MIT), Lexington, MA, USA, where he is currently a Member of the Technical Staff. His current research interests include MWPs, coherent photonic devices and subsystems, high-power waveguide photodiodes, high-power semiconductor optical amplifiers and their application in mode-locked lasers, and narrow-linewidth external-cavity lasers.

Dr. Yegnanarayanan is a member of the Optical Society of America (OSA).

Rajeev J. Ram (S'94–M'96–SM'07) received the B.S. degree in applied physics from the California Institute of Technology, Pasadena, CA, USA, in 1991, and the Ph.D. degree in electrical engineering from the University of California at Santa Barbara, Santa Barbara, CA, USA, in 1997.

He is currently a Professor with the Massachusetts Institute of Technology, Cambridge, MA, USA, where he is an Associate Director of the Research Laboratory of Electronics and Director of the Center for Integrated Photonics Systems. His research focuses on physical optics and electronics, including the development of novel components and systems for communications and sensing, novel semiconductor lasers for advanced fiber-optic communications, and studies of fundamental interactions between electronic materials and light.

Paul W. Juodawlkis (S'86–M'86–SM'06) received the B.S. degree from Michigan Technological University, Houghton, MI, USA, the M.S. degree from Purdue University, West Lafayette, IN, USA, and the Ph.D. degree from the Georgia Institute of Technology, Atlanta, GA, USA, all in electrical engineering.

From 1988 to 1993, he was a Technical Staff Member with the Massachusetts Institute of Technology (MIT) Lincoln Laboratory, Lexington, MA, USA, where he was a Hardware Systems Engineer involved with a multisensor airborne testbed program. He then joined the Ultrafast Optical Communications Laboratory (UFOCL), Georgia Institute of Technology. In 1999, he rejoined the MIT Lincoln Laboratory, as a member of the Electro-Optic Materials and Devices Group. He is currently an Assistant Group Leader of the Electro-Optic Materials and Devices Group, MIT Lincoln Laboratory, where he leads research on semiconductor opto-electronic devices and MWPs. His research efforts have focused on the development of optical sampling techniques for photonic analog-to-digital converters (ADCs), quantum-well electrorefractive modulators, high-power waveguide photodiodes, and high-power semiconductor optical amplifiers (SOAs) and their application in mode-locked lasers and narrow-linewidth external-cavity lasers.

Dr. Juodawlkis was general co-chair of the 2012 Conference on Lasers and Electro-Optics (CLEO) and program co-chair of the 2010 CLEO. He is currently a member of the IEEE Photonics Society Board of Governors (2011–2013). He was chair of the IEEE Photonics Society Technical Committee on Microwave Photonics (2003–2006), program co-chair of the 2003 Photonics Society Summer Topical Meeting on Photonic Time/Frequency Measurement and Control, and program committee member of the Optical Fiber Communication (OFC) Conference (2013) and the International Topical Meeting on Microwave Photonics (2004, 2008, 2013). He is a member of the Optical Society of America (OSA) and the American Association for the Advancement of Science (AAAS).